General Disclaimer

One or more of the Following Statements may affect this Document

- This document has been reproduced from the best copy furnished by the organizational source. It is being released in the interest of making available as much information as possible.

- This document may contain data, which exceeds the sheet parameters. It was furnished in this condition by the organizational source and is the best copy available.

- This document may contain tone-on-tone or color graphs, charts and/or pictures, which have been reproduced in black and white.

- This document is paginated as submitted by the original source.

- Portions of this document are not fully legible due to the historical nature of some of the material. However, it is the best reproduction available from the original submission.

NASA Technical Memorandum 83030

Measured and Calculated Wall Temperatures on Air-Cooled Turbine Vanes With Boundary Layer Transition

Curt H. Liebert, Raymond E. Gaugler, and Herbert J. Gladden
Lewis Research Center
Cleveland, Ohio

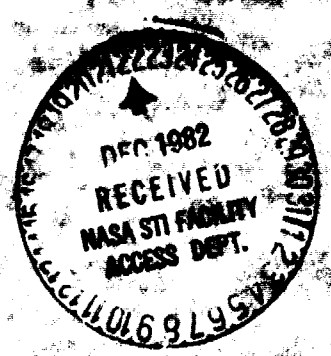

Prepared for the
Twenty-eighth Annual International Gas Turbine Conference
sponsored by the American Society of Mechanical Engineers
Phoenix, Arizona, March 27-31, 1983

NASA

MEASURED AND CALCULATED WALL TEMPERATURES ON AIR-COOLED TURBINE VANES WITH BOUNDARY LAYER TRANSITION

Curt H. Liebert, Raymond E. Gaugler, and Herbert J. Gladden
National Aeronautics and Space Administration
Lewis Research Center
Cleveland, Ohio

ABSTRACT

Convection cooled turbine vane metal wall temperatures experimentally obtained in a hot cascade for a given one-vane design were compared with wall temperatures calculated with TACT1 and STAN5 computer codes which incorporated various models for predicting laminar-to-turbulent boundary layer transition. Favorable comparisons on both vane surfaces were obtained at high Reynolds number with only one of these transition models. When other models were used, temperature differences between calculated and experimental data obtained at the high Reynolds number were as much as 14 percent in the separation bubble region of the pressure surface. On the suction surface and at lower Reynolds number, predictions and data unsatisfactorily differed by as much as 22 percent. Temperature differences of this magnitude can represent orders of magnitude error in blade life prediction.

INTRODUCTION

Improved component durability, lower maintenance costs, and reduced fuel consumption are major thrusts for advancing gas turbine engine technology. Improved durability of turbine components is dependent on effective cooling of vanes and blades, but at the same time, reduced fuel consumption requirements restrict the amount of bleed air available for cooling. The designers ability to meet these diverse goals is dependent on his knowledge of the heat transfer process in the turbine and his ability to predict component metal temperatures.

The verification of blade metal wall temperature predictions is very difficult because there is a lack of accurate and relevant experimental data for comparison purposes. Accurate prediction is imperative to the designer because at the nominal vane wall temperature of 1256 K, a four percent uncertainty in temperature (i.e., 35 percent error in heat transfer coefficient) results in a wall temperature error of 50 K and an order of magnitude decrement in vane life (1). Reference 1 discusses the parameters that can lead to uncertainty in the gas-side heat transfer coefficient calculations. Such factors as free stream turbulence, surface curvature, pressure gradients, and surface roughness can effect the level of heat flux through the boundary layer. Insufficient knowledge of these factors leads to substantial errors in calculating the gas-side heat transfer coefficients associated with the boundary layer transition region.

The limited scope of relevant experimental data is discussed by Reference 2. This reference describes experiments which were performed only in incompressible flow, and experiments where data were taken at ratios of gas-to-metal temperatures not typical of gas turbine practice. Many experiments were done without the use of a gas turbine combustor to set up temperatures and turbulence conditions similar to those in a gas turbine engine or were done with flat plates which do not set up transitional boundary layer flow in a manner typical of high pressure turbines. In addition, many of the relevant boundary conditions were unreported or were not measured. When predictive methods were tested against experiment in Reference 2, there were deviations in agreement of measured and calculated heat fluxes of 50 percent or more.

Our effort compares measured air-cooled metal vane wall temperatures with output from the best available codes incorporating a good definition of coolant passage geometry and boundary conditions, and presents an interim assessment of the codes. The experimental temperature data were obtained in a hot cascade facility at Lewis Research Center. Use of this cascade overcomes many of the inadequacies of the experiments described in Reference 2 by simulating the gas and coolant environment encountered in real turbine engines. The experimental data were taken over a range of gas-side Reynolds number, Re_c, based on chord length and mean exit condition of 1.1×10^6 to 3.6×10^6. Most of these tests were made at reduced conditions simulating current gas turbine engine operation at takeoff and cruise conditions. Wall temperatures were measured on two air-cooled vanes utilizing several internal cooling configurations at gas temperatures of 593 to 1552 K and gas pressures of 32.4 to 83.4 N/cm^2. Cooling air temperatures varied from 304 to 601 K.

Steady-state experimental vane temperatures were compared to vane temperatures calculated with a com-

puter program which combined the computer codes TACT1 (3) and STAN5 as modified according to Reference 4. The modified STAN5 code is a two-dimensional, finite-difference boundary layer code which was used to calculate hot gas-side heat transfer coefficient values for input to TACT1. Provision was made in the modified STAN5 to handle boundary layer transition. TACT1 is a quasi-three dimensional computer program for calculation of temperatures, pressures, heat transfer coefficients, and coolant flow in turbine vanes with cross flow impingement cooling, forced convection channel flow, or flow across arrays of pin fins, whichever is appropriate. For our report, TACT1 included a new impingement with cross flow heat transfer model developed under a NASA grant at Arizona State University (5).

EXPERIMENTAL TECHNIQUE

Cascade Facility

The hot cascade facility at the NASA Lewis Research Center is capable of operating at gas temperatures and pressures up to 1600 K and 100 N/cm^2. This facility consists of components which include an inlet section, a combustor section, a transition section, a vane test section (Fig. 1), and an exit section. The transition duct guides and accelerates the hot gas flow from the circular cross-section of the combustor to the annular inlet of the vane test section. The area ratio contraction is about 5 to 1. Typically, the gas temperature varied about ±2 percent over the vane midspan region. A detailed description of the hot cascade is given in Reference 6. Unpublished turbulence intensity measurements previously made with a single element hot-wire probe at gas temperatures of about 300 to 400 K showed that the turbulent intensity at the vane row inlet ranged from 6 to 10 percent.

Test Vanes

The turbine slave and instrumented test vanes used in this investigation were J-75-size airfoils (6) with impingement cooling the forward two-thirds of the airfoil and combined pin-fin and film cooling the aft one-third of the airfoil. The test vanes are identified in Figure 1 as numbers 2 and 3. A cross-sectional schematic of the airfoil and cooling configuration is shown in Figure 2. The vane geometry is given in Table I. Values of geometrical parameters described below were used as input to the calculations and were obtained from measurements on pieces of test vanes which were cut up after the tests were performed. Vane span was 9.78 centimeters and midspan chord length was 6.28 cm. Airfoil outer shell wall thickness at the midspan impingement cooled region was nominally 0.152 cm. Vane outer shell wall material was MAR-M-302.

The impingement insert had a staggered array of holes that were 0.051 cm in diameter. The hole spacing varied, depending on location, between 6.5 and 9 hole diameters spanwise and between 2.4 and 9 hole diameters chordwise. The closely spaced holes were in the leading-edge region (6.5 by 2.4); the midchord region had larger spacings (9 by 9 on the pressure side and 8.5 by 8.5 on the suction side). The spacing between the insert and the shell wall was approximately 1.5 hole diameters in the midchord region and approximately 2 hole diameters in the leading-edge region. The impingement insert material was L-605.

There were seven chordwise rows of round pin fins in the split trailing edge of each vane (Fig. 2). The three upstream rows had pin diameters of approximately 0.102 cm with a spanwise spacing of 0.406 cm and a chordwise spacing of 0.353 cm. The last four rows had pin diameters of 0.076 cm with a spanwise spacing of 0.305 cm and a chordwise spacing of 0.264 cm. The width of the split-trailing-edge channel at the point of discharge was 0.089 cm.

A single row of cooling holes on the vane pressure surface (Fig. 2) ejected air at an angle of 30° to the vane surface in the spanwise direction. The purpose of these holes was to provide a sufficient flow area to accommodate the design coolant flow requirements.

Test Conditions

Table II represents the experimental conditions at which the wall temperature measurements were made as-well-as the aircraft type and associated flight conditions which these tests simulate. The cascade was operated at Reynolds numbers, Re_c, of 1.1×10^6 to 3.6×10^6 based on chord length and mean exit conditions. To achieve increasing Re_c, gas temperatures were usually decreased from a high value of 1552 K to a low value of 593 K (Table II). The pressure range needed to set the various Re_c varied from 32.4 to 83.4 N/cm^2 (Table II). The cascade was operated at a constant expansion ratio resulting in a mean exit velocity ratio of 0.85. Gas inlet temperature and pressure surveys were made for each data point. The vane temperatures were recorded with the survey probe removed from the gas stream.

Instrumentation

The instrumentation provided detailed information about cascade gas-stream temperatures and mass flow rates, vane inlet cooling air temperature and mass flow rate, and local midspan vane metal temperatures. Figure 1 shows the location of the instrumentation used in the hot gas stream at the inlet to the annular sector of the vane test section. At station 1, a radial traversing total temperature probe was located in front of channel 3 and a spanwise traversing total pressure probe was located in front of channel 4. These probes were used to obtain average inlet gas conditions to the cascade. Static pressures were also measured at the exit mid-channel position of channels 2, 3 and 4 and at both vane inner and outer radius platforms at station 2. These pressures were used to establish the midstream exit critical velocity ratio. Further details are given in Reference 6.

The metal shell wall of each of the two air-cooled test vanes (numbers 2 and 3 in Fig. 1) were instrumented with 12 Chromel-Alumel thermocouples in the midspan region. Figure 2 shows the location of these thermocouples. Details on the thermocouple fabrication are given in Reference 7. The thermocouples were placed in rectangular grooves machined into the vane metal walls. Then the thermocouple hot junctions were spotwelded to the bottom of the grooves. The void above the junction was filled with a contoured metal slug to aid in restoring the undisturbed isothermal patterns of the airfoil. Finally, a cover plate was spotwelded over the grooves and dressed down to the aerodynamic profile.

Following gas-turbine engine practice, cooling air was supplied to test vanes 2 and 3 (Fig. 1) from a single plenum attached to the airfoil sections. The flow was measured with a venturi-type flow meter.

Prior to entering the manifold, the air was filtered by a 5 mm sintered-element filter. Cooling air temperatures were measured with thermocouples located in the plenum.

Static Pressure Distributions

Vane surface static pressure distributions on two uncooled vanes with aerodynamic profiles identical to those of the vanes used in this investigation were obtained from Reference 6. These distributions were taken at gas temperatures of 307 to 728 K and are presented in Figure 3 as a ratio of static pressure to total pressure versus x/L. The variable, x, is the surface distance along the vane from the leading edge stagnation point and L is the total surface distance from the leading edge to the trailing edge stagnation points. The experimental data in Reference 6 shows that the flow over test vane 3 expands to a lower pressure in the suction surface throat region than does the flow over test vane 2. There was about a five percent difference in pressure ratio values at this location. The pressure ratio values were comparable between vane 2 and vane 3 within ±1 percent at all other locations.

ANALYSIS

Hot Gas-Side Boundary Layer Calculations Using Analysis of References 3 and 4

Leading edge boundary layer. - The hot gas-side boundary layer calculations on the vanes were started at the stagnation point by using the modification to the STAN5 code described in Reference 4. This modification, based on correlation of experimental Nusselt number data (4), involved addition of a subroutine to STAN5 for calculating steady-state boundary layer heat transfer coefficients around a cylinder in laminar crossflow. These coefficients were then faired into heat transfer coefficients calculated with STAN5 at locations aft of the cylindrical leading edge by assuming either laminar boundary layer transition to turbulent flow or a continuation of the laminar boundary layer.

Attached boundary layer transition aft of the leading edge. - STAN5 calculations for heat transfer coefficients at vane surface locations aft of the leading edge require velocity distribution inputs along both the suction and pressure surfaces. These distributions were calculated from the experimental gas-side static pressure to total pressure ratio data shown in Figure 3. For convenience, the velocity calculations were done by assuming isentropic, perfect gas conditions and also by assuming that the static pressure normal to the wall was constant throughout the boundary layer and into the free stream. This assumption may not give accurate wall temperature prediction in separated or transitional flow, or in the leading edge region.

Several empirical models are provided in STAN5 for describing the transition of the boundary layer from laminar to turbulent flow. These models assume that the boundary layer is attached to the surface. The start of transition was modeled using correlations of either Seyb (8), Dunham (9), or Van Driest and Blumer (10); these models are designated herein as model numbers 1, 2, or 3, respectively. The model for the length of transition from laminar to turbulent flow was taken from Dhawan and Narasimha (11).

Separated boundary layer transition aft of the leading edge. - Sometimes STAN5 boundary layer flow calculations will indicate laminar flow separation before the start of transition can be calculated. When separation is predicted the program cannot calculate through it, and so the method described in Reference 4 was used with modified STAN5 to force the transition of a short, separated boundary layer into an assumed, attached turbulent boundary layer condition which will prevail along the remaining vane surface downstream of the attachment point. A limited separated flow region of this kind is called a bubble (12). The procedure for modeling this region is called "trip to turbulence" and the model identification herein in number 4.

Thermal Analysis of the Vane

The hot gas-side heat transfer coefficients calculated with modified STAN5 are used as boundary conditions for the TACT1 program. As described in Reference 3, the calculation is performed by sectioning the vane into chordwise constant-height slices. For each vane slice, three-dimensional heat conduction equations were solved in the metal wall. Then for each vane slice, values of local impingement cooling flow rates and heat transfer coefficient parameters were calculated on a one dimensional basis. Initially, TACT1 calculations were done using five slices and the midspan results were compared to the same case using only one slice. The difference in analytical results was within ±1 percent which was assumed to be acceptable since this is within the accuracy of the experimental data.

The coolant flow rates and heat transfer coefficient parameters were calculated by using an impingement with crossflow model for staggered arrays developed under a NASA grant at Arizona State University (5). The experimentally determined coolant flow rate was used as input to the impingement model. Output from TACT1 included metal temperatures calculated at the hot-junction position of the thermocouples mounted in the vane walls. Heat flux through the vane walls and to the coolant is a function, among other things, of the temperature differences between the hot gas and the wall, of the cooling air and wall temperature differences, and cooling air and hot gas velocities. The heat fluxes, temperature differences, and velocities varied as Re_c was set at values of 1.1×10^6 to 3.6×10^6 in the cascade. Spot calculations indicated that the variations had only a 1 to 2 percent effect on the film heat transfer coefficients when gas or coolant boundary layer thermal conductivities, specific heats and viscosities were evaluated at either a reference enthalpy, a reference temperature, or a arithmetic average temperature between hot gas and wall, or coolant and wall. Therefore, for convenience, thermodynamic and transport properties of air and/or its products of combustion with ASTM-A-1 fuel (13), were evaluated at the average temperature condition.

RESULTS AND DISCUSSION

Results Applicable to Both Suction and Pressure Surfaces

Measured values of wall temperatures versus x/L are presented in Figures 4(a) to (f) for increasing values of Re_c. For clarity, Figures 4(d) to (f) have an expanded temperature scale. The two test vanes performed experimentally in a similar but not identical manner. Wall temperature measurement differences at corresponding locations on the two vanes were within ±5 percent. Because these variations are minimal, the average values (denoted by the solid

lines in Fig. 4) do not mask the variations of wall temperature associated with the laminar, transitional and turbulent character of the boundary layer flow along the vane walls.

The 0 to ±5 percent measured temperature differences obtained at corresponding locations (i.e., the precision of measurement within a range of 0 to ±5 percent) are probably due to: (1) variations in local coolant flow rates caused by deformation of cooling flow passages at elevated temperatures, (2) differences in the static pressure on the two vanes which can lead to differences in heat flux to the vanes at corresponding locations and at different coolant flow rates, and (3) variations in flow along the channels between the vanes.

The measured wall temperatures at corresponding vane locations are rather small because care was taken in design and fabrication of the cascade and in selection of the matched test vanes. Because of this attention to detail, about half of the data fall within a two percent precision range needed for very precise comparison of theory and experiment.

Comparisons of calculated and measured convection-cooled vane wall temperatures are presented in Figures 5(a) to (c) for $Re_c = 1.1x10^6$, $1.3x10^6$, and $3.6x10^6$. The measured data presented in these figures is the same as that presented in Figures 4(a), (b), and (f), respectively. The comparison is meant to be qualitative in the sense that it shows for this vane design, only, the impact of selecting the various transition boundary layer flow models and then proceeding with boundary layer and associated heat transfer calculations for cooled metal wall temperature over the aerodynamic surfaces of the vanes. Prediction of metal wall temperature was the most difficult in the transition region, and was reasonably good (0 to 5 percent) at the leading edge region of our vanes operating in our cascade.

Suction Surface

Figure 3 shows that the suction surface pressure gradient is favorable from the stagnation line to the throat location. Therefore, it is highly probable that the boundary layers will be attached to the convection-cooled suction surface at the hot-gas conditions of these experiments (12).

Figure 5(a), which presents results at $Re_c = 1.1x10^6$ (simulated supersonic transport aircraft flight conditions, Table II) shows that the measured wall temperatures decrease with increasing x/L. The values agreed within 4 percent of values calculated with modified STAN5 when it was assumed that the boundary layer aft of the leading edge is fully laminar and attached to the surface. Conversely, when attached boundary layer transition models 1, 2, or 3 are used, figure 5a shows much poorer agreement of the mathematical descriptions and the experimental wall temperature observations. These three models predicted that transitional flow will start at x/L equal to about 0.1 to 0.2 and that wall temperatures increase and level off as x/L gets bigger. Since the experimental temperature data decrease over most of the vane surface with increasing x/L, it is seen that the transition models predict transition to turbulent flow at too short a distance from the stagnation point. This leads to calculated wall temperature values which are 15 to 22 percent higher than the measured values. Figure 5a also shows that turbine cooling suction surface designs incorporating the codes used herein would result in vanes which were reasonably uniformly cooled in the chordwise direction for probable achievement of satisfactory turbine vane life, when in reality the vane could have a large temperature gradient along the suction surface which could lead to excessive thermal stresses and premature vane distress in actual engine operation.

As shown in Figure 5(b), which gives results at a Re_c setting of $1.3x10^6$, all of the models used for describing the transition of attached boundary layer flow again predicted transition at too short a distance from the stagnation line. Predictions were 20 percent higher than measurement values at x/L greater than about 0.1 to 0.2. Also shown in Figure 5(b) is the modified STAN5 fully laminar calculation which is 18 percent lower than the measurements. This suggests that although the boundary layer has not yet reached a transitional state at this higher Re_c, it nevertheless is probably less stable (12) or less laminar-like than the boundary layer established at gas conditions corresponding to $Re_c = 1.1x10^6$ (fig. 5a).

Transition from laminar to turbulent flow occurs on the surface when Re_c becomes sufficiently high to allow instablities in the boundary layer to grow (12). Figure 4(d) suggests that transition is starting at $Re_c = 1.9x10^6$. Figures 4(e) and (f) show that transition to turbulence is finally accomplished at Re_c settings in the range of $2x10^6$ to $3.6x10^6$. The experimental and calculated metal wall temperatures were compared in Figure 5(c) at the highest Re_c equal $3.6x10^6$ where transition is accomplished. The resultant low wall temperature of 450 to 500 K comes about because of the necessity of lowering the gas temperature to 593 K so that this value of Re_c could be set in our cascade. This Re_c is the same as the takeoff and landing Re_c developed in conventional engines (Table II). The comparison qualitatively shows agreement within 4 percent using transition models 1, 2, or 3. For more insight into the physics of these heat transfer problems, other experiments are needed so that comparisons at both high wall temperatures and high Reynolds number settings can be made. (For clarity, Fig. 5(c) has an expanded temperature scale.)

Pressure Surface

Figure 3 shows an adverse pressure gradient at x/L of about 0.08 to 0.18. Reference 12 points out that an adverse pressure gradient can (but not always) be associated with a separated boundary layer.

Figure 5(a) presents results for gas conditions corresponding to the lowest Reynolds number setting, $Re_c = 1.1x10^6$ and high values of wall temperature. The data and calculations using transition models 2 and 3 for attached boundary layer flow correspond to within 7 percent. Transition model 1 could not be used because it predicted separation would occur ahead of the location for the start of transition; this suggests that model 4 might also be applicable. As shown in figure 5a, the use of model 4 predicted wall temperatures which were within 7 percent of the experimental data. Thus, calculations based on models dealing with the different transition concepts of attached (models 2 and 3) and bubble (model 4) boundary layer flow are both somewhat good agreement with the temperature measurements. Probably the reason for the somewhat good agreement is that models 2 and 3 as well as model 4 predict short transition lengths followed by turbulent, attached boundary layers downstream of the transition region.

Only model 4 was applicable for predicting the experimental air-cooled metal wall temperatures shown

in Figure 5(b) at an Re_c setting equal to 1.3×10^6 and high values of wall temperature. Figure 5(b) shows that agreement between calculated and measured wall temperatures was within 15 percent in the transition region. Agreement at other locations fore and aft of the transition region along the pressure surface was about 5 percent.

Figure 5(c) presents pressure surface results for the highest Re_c setting at 3.6×10^6 and the figure shows agreement of experimental and calculated wall temperatures (400 to 500 K) within 5 percent using model 3. The wall temperature correspondence was poorer when models 2 and 1 were incorporated; agreement in the transition region was 10 and 14 percent, respectively. Clearer understanding of the heat transfer phenomenon may be gained when experiments are performed at higher wall temperatures.

Examples of calculated values of gas side heat transfer coefficients are given in Figure 6 but were not compared with experiment because experimental values could not be measured. Heat flux gages for accurate determination of heat transfer coefficients on vanes operating at high temperatures and pressures were not available.

SUMMARY AND CONCLUSIONS

Considerable attention to detail was given to the aerodynamic design, fabrication, and instrumentation of the NASA Lewis cascade test section. In addition, a great deal of care was extended in the selection of matched test vanes and in the installation of thermocouples for accurate temperature measurement. As a result of this careful attention to detail, about half of the wa temperature values measured at corresponding positions on the two air-cooled test vanes agreed within ±0 to 2 percent and the other half of the paired measurements agreed within ±5 percent of the line drawn through the average of the paired values. This precision was needed for meaningful comparison of measured and calculated wall temperatures.

The accuracy of prediction depended highly on the Reynolds number, transition model, surface and location. On the suction surface the best comparison occurred at the highest Reynolds number setting of 3.6×10^6 and lowest metal wall temperature. For this condition boundary layer transition models 1, 2, and 3 along with STAN5 and TACT1 predicted metal temperatures within 4 percent of the experimental values. Significantly, these particular experimental values differed by only about 2 percent at corresponding locations on each of the two vanes (Fig. 4(f)). This is the best analytical agreement with experiment that could be achieved on a given aerodynamic surface using carefully measured values of velocity distribution along the surface, vane wall temperature and thickness values, and values of coolant passage geometry parameters for input to the computer codes.

The difficulty of predicting suction surface metal wall temperatures becomes obvious from comparison of calculation and experiment at the lower Reynolds number settings and higher wall temperatures where transition models 1, 2, and 3 predict transition to turbulent flow at too short a distance from the stagnation point. This leads to calculated suction surface wall temperature values which are 15 to 22 percent higher than the measured values. These differences between measured and calculated vane wall temperatures represent orders of magnitude er or in blade life prediction. Such poor agreement between calculated and measured values in the boundary layer transition region was also observed on the pressure surface. Thus, considerable improvement in transition boundary layer theory is needed before computer codes can be considered reliable in predicting airfoil temperature over a full range of conditions.

It is recognized that the cost of obtaining precise and accurate cooled blade metal temperatures experimentally for design purposes is high and that the exclusive use of computer codes as a design tool could lower costs. However, our research suggests that the exclusive use of computer codes for design purposes can not yet be fully justified until heat transfer prediction in the transition boundary layer is improved. So for the present, experiment is necessary for the cooled turbine design process and for the verification of design codes.

REFERENCES

1. Graham, R. W., "Fundamental Mechanisms That Influence the Estimate of Heat Transfer to Gas Turbine Blades," NASA TM-79128, 1979.
2. Daniels, L. D., and Browne, W. B., "Calculation of Heat Transfer Rates to Gas Turbine Blades," International Journal of Heat and Mass Transfer, Vol. 24, No. 5, May 1981, pp. 871-879.
3. Gaugler, R. E., "TACTI, A Computer Program for the Transient Thermal Analysis of a Cooled Turbine Blade or Vane Equipped With a Coolant In- sert," NASA TP-1271, 1978.
4. Gaugler, R. E., "Some Modifications to, and Operational Experiences With, the Two-Dimensional, Finite-Difference, Boundary-Layer Code, STAN5," ASME Paper 81-GT-89, Mar. 1981.
5. Florschuetz, L. W., Metzger, D. E., and Truman, C. R., "Jet Array Impingement With Crossflow - Correlation of Streamwise Resolved Flow and Heat Transfer Distributions," NASA CR-3373, 1981.
6. Gladden, H. J., et. al., "Aerodynamic Investigation of Four-Vane Cascade Designed for Turbine Cooling Studies," NASA TM X-1954, 1970.
7. Holanda, R., Glawe, G., and Krause, L., "Miniature Sheathed Thermocouples for Turbine Blade Temperature Measurement," NASA TN D-7671, 1974.
8. Seyb, N. J., "The Role of Boundary Layers in Axial Flow Turbomachines and the Prediction of Their Effects," Boundary-Layer Effects in Turbomachinery, AGARD-AG-164, 1972, pp. 241-259.
9. Dunham, J., "Prediction of Boundary-Layer Transition on Turbomachinery Blades," Boundary-Layer Effects on Turbomachinery, AGARD-AG-164, 1972, pp. 55-71.
10. Van Driest, E. R., and Blumer, C. B., "Boundary Layer Transition: Free-stream Turbulence and Pressure Gradient Effects," AIAA Journal, Vol. 1, No. 6, June 1963, pp. 1303-1306.
11. Dhawan, S., and Narasimha, R., "Some Properties of Boundary Layer Flow During the Transition From Laminar to Turbulent Motion," Journal of Fluid Mechanics, Vol. 3, No. 4, Jan. 1958, pp. 418-436.
12. Cebeci, T., and Bradshaw, P., Momentum Transfer in Boundary Layers, Hemisphere Publishing Corp., Washington, 1977.
13. Hippensteele, S. A., and Colladay, R. S., "Computer Program for Obtaining Thermodynamic and Transport Properties of Air and Products of Combustion of ASTM-A-1 Fuel and Air," NASA TP-1160, 1978.

TABLE I - VANE GEOMETRY

Tip radius	10.50 cm
Hub radius	30.72 cm
Hub-to-tip radius ratio	0.76
Vane height	9.78 cm
Vane chord	6.28 cm
Vane solidity	2.05
Aspect ratio	1.54
Leading edge diameter	0.813 cm

TABLE II - EXPERIMENTAL CONDITIONS[a]

Fig. No.	Reynolds number based on chord Re_c	Static pressure free stream N/cm^2	Gas temperature, K	Cooling air temperature, K	Cooling air flow kg/sec	Mass Flow coolant percent mass flow gas	Aircraft type and flight conditions	Reynolds number based on leading edge diameter
4a 5a	1.1×10^6	32.4	1267	601	0.00108	0.022		4.9×10^4
4b 5b	1.3×10^6	83.4	1552	307	0.0133	0.0293	SST[b] (takeoff)	5.9×10^4
4c	1.7×10^6	59.6	921	304	0.06305	0.0326	CTOL[d] (cruise)	7.8×10^4
4d	1.9×10^6	64.8	933	454	0.0282	0.0268	VTOL[c] (cruise)	8.5×10^4
4e	2.0×10^6	71.0	946	307	0.04944	0.0406		9.0×10^4
4f 5c	3.6×10^6	71.7	593	308	0.04481	0.0306	CTOL[d] (takeoff)	1.55×10^5

[a] Estimated turbulence level was 6 to 10 percent for all experimental conditions.

[b] SST - Supersonic transport engine.

[c] VTOL - Vertical takeoff and landing engine.

[d] CTOL - Conventional takeoff and landing engine.

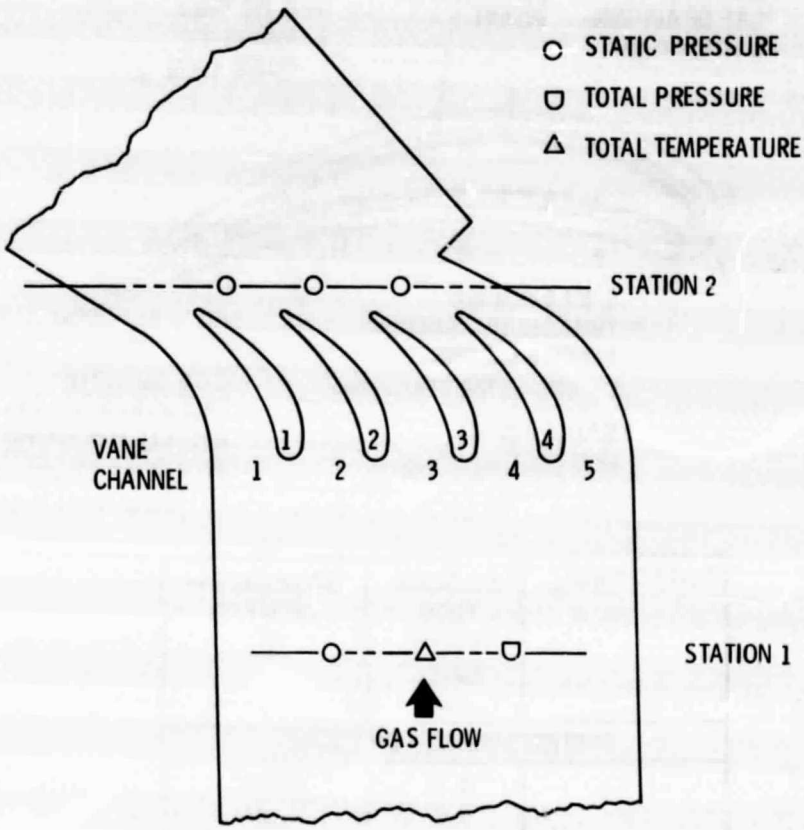

Figure 1. - Schematic top view of vane test section.

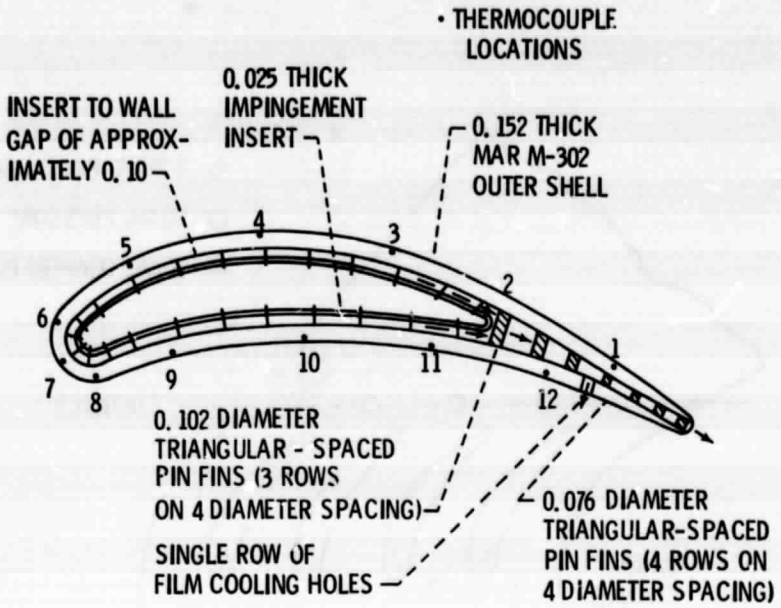

THERMOCOUPLE	DISTANCE FROM LEADING EDGE, cm	DIMENSIONLESS DISTANCE X/L
SUCTION SURFACE; L = 7.42 cm		
1	6.42	0.866
2	5.07	.684
3	3.88	.523
4	2.60	.351
5	1.32	.178
6	.50	.067
7	0	0
PRESSURE SURFACE; L = 6.45 cm		
8	0.39	0.061
9	1.25	.194
10	2.52	.391
11	3.78	.586
12	4.85	.752

Figure 2. - Schematic cross-sectional midspan view of test vane, showing the internal cooling configuration and the thermocouple locations.

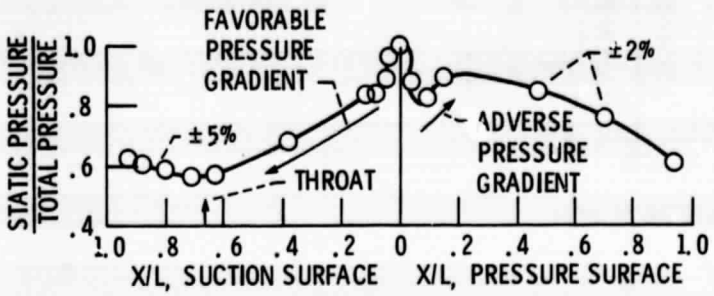

Figure 3. - Experimental pressure distribution.
Re = 1.3x10^6 to 1.7x10^6 (reference 7).

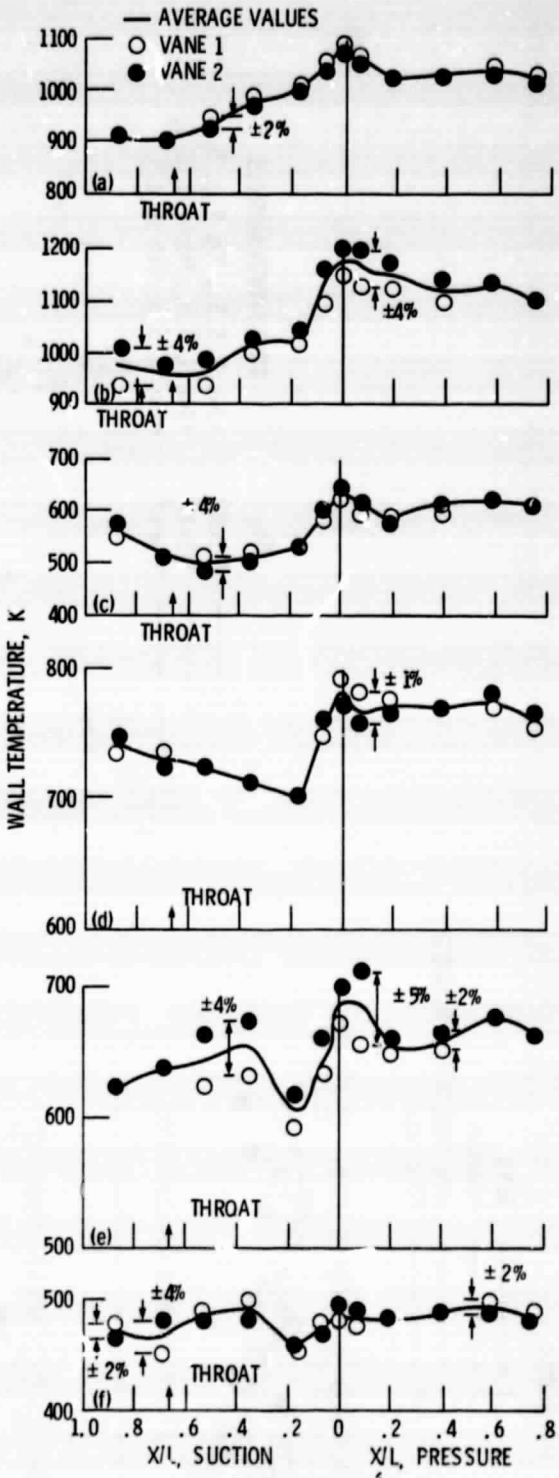

(a) Re_c = 1.1x10^6.
(b) Re_c = 1.3x10^6.
(c) Re_c = 1.7x10^6.
(d) Re_c = 1.9x10^6.
(e) Re_c = 2x10^6.
(f) Re_c = 3.6x10^6.

Figure 4. - Temperature distributions.

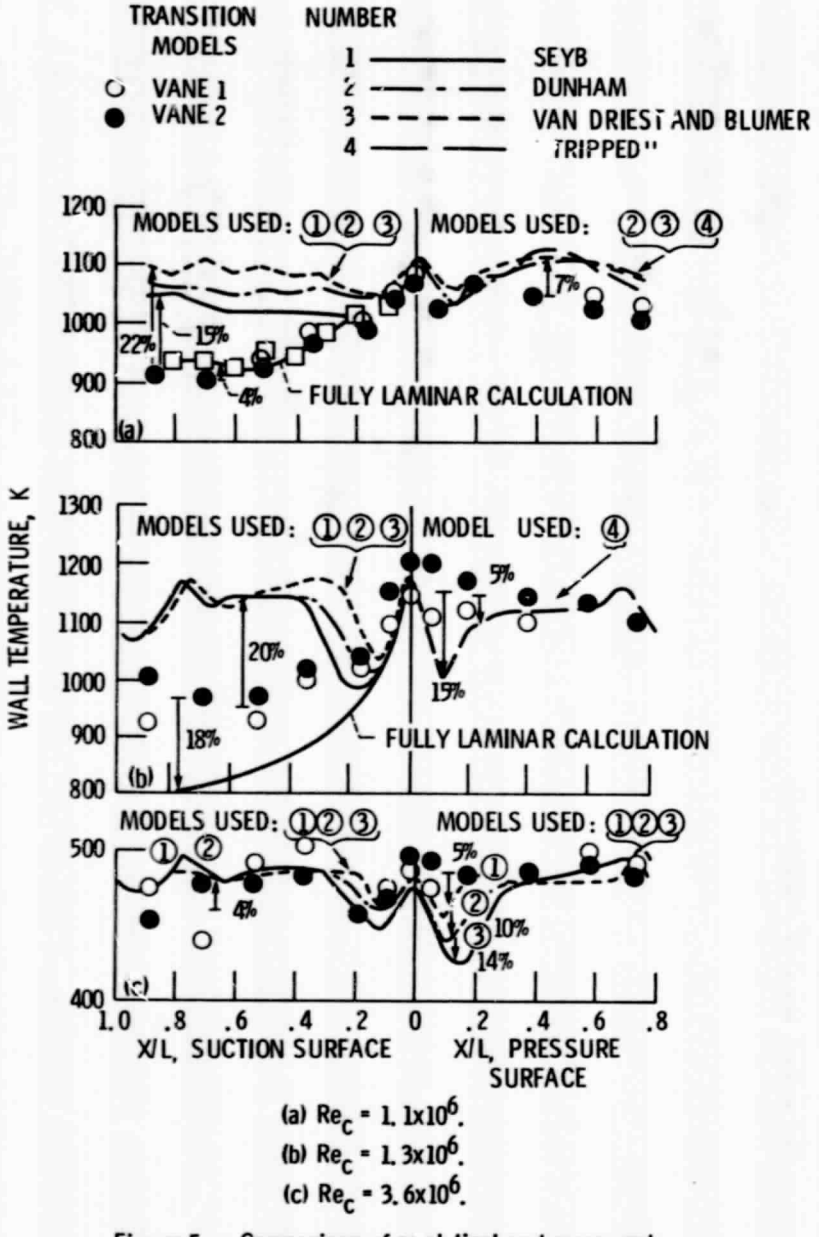

(a) $Re_c = 1.1 \times 10^6$.
(b) $Re_c = 1.3 \times 10^6$.
(c) $Re_c = 3.6 \times 10^6$.

Figure 5. - Comparison of analytical and measured wall temperatures.

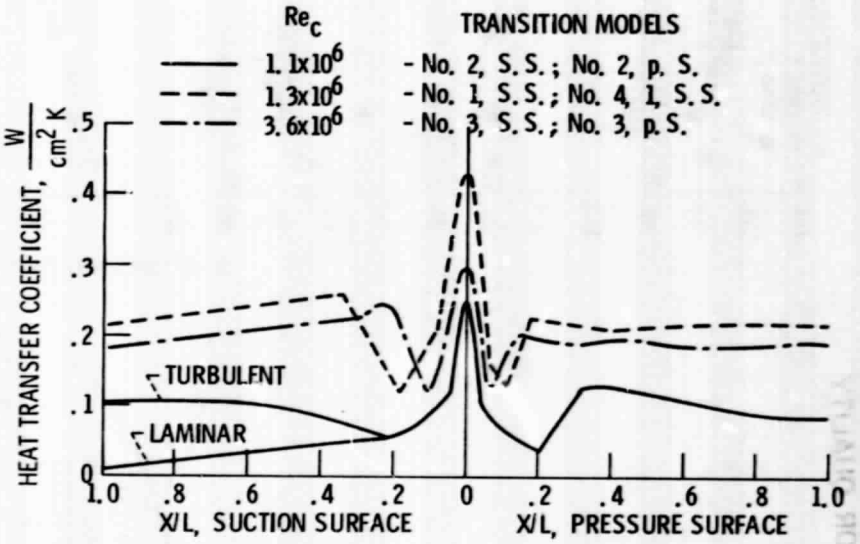

Figure 6. - Examples of calculated gas-side heat transfer coefficients.